

**NASA TECHNICAL
MEMORANDUM**



NASA TM X-1546

NASA TM X-1546

GPO PRICE \$ _____

CSFTI PRICE(S) \$ _____

Hard copy (HC) 3.00

Micro fiche (MF) 6.5

653 July 65

FACILITY FORM 602

(ACCESSION NUMBER)

(PAGES)

(NASA CR OR TM OR AD NUMBER)

(THRU)

(CODE)

(CATEGORY)

**1/14.2-SCALE INVESTIGATION
OF SUBMERGED NOZZLE FOR
SL-3 260-INCH SOLID ROCKET**

by Reino J. Salmi and James J. Pelouch, Jr.

Lewis Research Center

Cleveland, Ohio

1/14.2-SCALE INVESTIGATION OF SUBMERGED NOZZLE
FOR SL-3 260-INCH SOLID ROCKET

By Reino J. Salmi and James J. Pelouch, Jr.

Lewis Research Center
Cleveland, Ohio

NATIONAL AERONAUTICS AND SPACE ADMINISTRATION

For sale by the Clearinghouse for Federal Scientific and Technical Information
Springfield, Virginia 22151 - CFSTI price \$3.00

1/14. 2-SCALE INVESTIGATION OF SUBMERGED NOZZLE

FOR SL-3 260-INCH SOLID ROCKET*

by Reino J. Salmi and James J. Pelouch, Jr.

Lewis Research Center

SUMMARY

As a result of the investigation reported in reference 1, the original submerged nozzle configuration for the SL-3 260-inch solid propellant rocket was modified to provide additional insulation and protection against the erosive effects of hot exhaust gases in the annular channel between the submerged nozzle lip and the rocket aft-end casing. Tests of the modified nozzle design indicated that the circumferential flow velocities in the annular channel were lower for the modified nozzle than for the original configuration for the case of an unburned or 100-percent grain. For the case of the 34-percent regressed grain, which reduced the flow velocities in the annular channel, flow Mach numbers approximately equal to those of the original nozzle were obtained with the modified nozzle.

INTRODUCTION

As an initial phase in the development of a gimbaling nozzle for the 260-inch solid rocket, a partially submerged convergent-divergent nozzle was designed for the SL-3 motor. The SL-3 test firing was intended to determine the aerodynamic performance of a nongimbaling version of the nozzle design and the durability of its ablative surface. A small-scale compressed-air model investigation of the original submerged nozzle design (ref. 1) revealed that the exhaust flow from the clover-leaf-shaped propellant grain port induced a turbulent high-velocity circumferential flow in the annular clearance channel between the submerged nozzle entrance lip and the aft-end rocket casing. Because the initial nozzle design was based on stagnant flow conditions in the annular channel, modifications were made to the initial design to protect this region from the erosive effects of the hot exhaust gases. Reported herein are the results of tests with the small-scale model to determine the flow characteristics in the annular channel with the modified nozzle.

*Presented at Second AIAA-ICRPG Solid Propellant Conference, Anaheim, California, June 1967.

The tests were made at the Lewis Research Center in an ambient pressure test facility using compressed air (ref. 1). A new nozzle was used which conformed to the final SL-3 nozzle configuration. The flow directions and velocities in the annular channel were determined from tuft studies and measurements of the static and total pressures.

APPARATUS

The 1/14.2-scale compressed air model of the Aerojet-General 260-inch solid propellant rocket used in the tests of reference 1 was investigated with a new nozzle which simulated the final nozzle design for the SL-3 rocket. Figure 1 presents a cross section of the SL-3 nozzle and indicates the modifications to the original design. The primary change in the nozzle contour was the reduction in the annular channel caused by the additional polybutadiene acrylonitrile (PBAN) insulation material. As in the case of the original tests (ref. 1), the nozzle was cut off 3/4-inch (0.019m) downstream of the throat for convenience because the divergent exit cone does not affect the flow upstream of the nozzle throat.

The model tests were made in an atmospheric test facility shown in figure 2. The compressed air used to simulate the rocket exhaust gases was brought to the annular chamber between the simulated propellant grain and the model outer shell through a 6-inch pipe which entered the model side near the closed end. The model was operated at a chamber pressure of 30 psia (0.2064 MN/m²).

High-speed movies of the motions of wool tufts cemented to the channel walls indicated the flow directions in the annular channel. A transparent aft-end casing was used to permit visual observation. The transparent aft-end casing and the steel nozzle (figs 3 and 4), comprised the model aft-end assembly.

The flow velocities in the annular channel and on the nozzle surface were determined from measurements of the local static and total pressures. One radial row of orifices was installed and the model aft-end assembly was rotated relative to the simulated propellant grain to obtain circumferential measurements. The pressures were measured with mercury and tetrabromoethane (TBE) manometer boards and recorded photographically. The total pressure probe in the annular passage could be remotely rotated to obtain the true total head. The heading of the total probe also indicated the direction of flow in the annular channel at that point.

To simulate the uniform emanation of burning gases from the surface of the solid propellant grain, simulated model grains were fabricated from sheet steel with uniformly spaced 3/16-inch (0.0048-m) diameter holes. The total hole area was about 40 percent of the nozzle throat area to assure choking of the holes and thereby provide uniform air distribution. To avoid having high-speed air jets from the grain lobe ends blowing directly into the nozzle lip and annular channel region, the air to the grain lobe ends was supplied through a bulkhead with metering orifice holes. The grain lobe ends were made with

many small holes which allowed the simulated exhaust to emanate more uniformly and at a much lower velocity. Shown in figure 5 are the simulated propellant grains. The 100 percent or unburned grain shown on the left is the type of grain used in the SL-3 rocket. The flat ends of the grain lobe slant inward 30° from a normal to the model centerline. The grain shown on the right simulated the condition where the grain has regressed 34 percent due to burning. The grain lobes are considerably smaller and the port area enlarged. The grain port geometry is described in figure 6.

RESULTS AND DISCUSSION

The flow characteristics in the annular channel between the submerged nozzle lip and the aft-end casing obtained with the modified nozzle contour are compared to those of the original SL-3 nozzle in figures 7 and 8. Presented in figure 7 are the flow directions and Mach number contours obtained with the simulated unburned or 100 percent grain. The flow directions in the annular channel (as shown by the arrows) were unchanged by the nozzle modifications, as would be expected. The flow entered the channel in the region between the grain lobes and exited directly behind the lobes. The flow Mach numbers, on the other hand, were substantially lower for the modified nozzle. Evidently the shallower passage of the modified nozzle was less conducive to a well established circumferential flow from the high pressure stagnation region between the grain lobes to the low base pressure region behind the grain lobes. As in the case of the initial nozzle, the annular channel flow was extremely turbulent.

The results obtained with the 34 percent regressed grain are shown in figure 8. The original nozzle tests (ref. 1) indicated a large decrease in the annular channel flow velocities due to the grain regression. For the modified nozzle, the annular channel Mach numbers were also reduced by the regressed grain, but the incremental reduction was much less than in the case of the original nozzle. However, the Mach numbers for the modified nozzle with the regressed grain are of such a magnitude that ablative erosion in this region should be low.

For the modified nozzle and the regressed grain, the circumferential flow in the annular channel exited in a region slightly to one side of the grain lobes rather than directly behind them. The induced flow patterns in annular channels are sensitive to small disturbances and this effect is attributed to a circumferential component of flow from the simulated grain port. Examination of the simulated grain revealed that many of the small grain perforations exhibited a slight misalignment in a direction such that a rotational velocity component was induced. The 34-percent regressed grain used in the tests of reference 1 with the original nozzle did not have a perforated grain surface. In this case, the air to the regressed grain was introduced into the grain port from three large holes near the grain head end, and no circumferential flow was observed.

Tests with the original nozzle indicated that the three-lobed grain port also caused a distortion of the flow through the nozzle. Similar results were obtained

with the modified nozzle. The circumferential variations of the nozzle surface Mach numbers at two nozzle stations are shown in figure 9. At station 1, which corresponds to the nozzle throat (fig. 1), a very slight increase in Mach number occurred in the region directly behind the grain lobe, with the 100-percent grain. No distortion was measured with the 34-percent grain. At station 2, which was located upstream in the convergent section of the nozzle where the Mach number was about 0.5, a circumferential variation in Mach number in excess of 0.1 occurred with the 100-percent grain, with the lower Mach numbers occurring directly behind the grain lobes and the highest Mach numbers in the region directly between the lobes. Again with the 34-percent grain, relatively little circumferential distortion occurred.

The flow Mach numbers at the nozzle throat surface as indicated by figure 9 are in the supersonic flow range at values greater than those normally associated with a curved sonic line at the throat. Both the highly turbulent flow from the porous simulated grain (as evidenced by the movies of the tuft behavior in the annular channel) and the abrupt turning of the flow as it approached the nozzle entrance contribute to the formation of a turbulent boundary layer in the nozzle entrance. The flow acceleration in the nozzle entrance apparently has an effect of thinning out the turbulent boundary layer, especially near the nozzle throat. At somewhat lower Reynolds numbers (0.9×10^6 compared to 5.6×10^6) actual reverse transitions from turbulent to laminar boundary layers have been observed in the throat region for rapidly accelerating flows. A rapidly decreasing boundary layer displacement thickness associated with the thinning turbulent boundary layer could create an effective throat ahead of the physical throat and allow the flow to expand to the observed supersonic Mach numbers. The nozzle entrance boundary layer phenomena referred to here is discussed in detail by Bartz in reference 2.

The results of the actual firing of the SL-3 rocket on June 17, 1967 indicated that the areas of concern in the annular channel successfully withstood the full duration test.

SUMMARY OF RESULTS

Small-scale compressed air model tests of the final submerged nozzle configuration for the SL-3 260-inch solid propellant rocket indicated that:

1. With a simulated unburned or 100-percent grain, the circumferential flow velocities induced in the annular channel between the submerged nozzle lip and the rocket aft-end casing by the asymmetric grain port were lower for the modified nozzle than for the original nozzle.
2. As in the case of the original nozzle, the induced circumferential velocities in the annular channel were reduced by the 34-percent regressed grain to the point where ablative erosion should be no problem.

Lewis Research Center,
National Aeronautics and Space Administration,
Cleveland, Ohio, December 4, 1967,

REFERENCES

1. Salmi, Reino J.; and Pelouch, James J., Jr.: Investigation of a Submerged Nozzle on a 1/14.2-Scale Model of the 260-Inch Solid Rocket. NASA TM X-1388, 1967.
2. Bartz, D. R.: Turbulent Boundary-Layer Heat Transfer from Rapidly Accelerating Flow of Rocket Combustion Gases and of Heated Air. Advances in Heat Transfer. Vol. 2. J. P. Hartnett and T. F. Irvine, Jr., eds., Academic Press, 1965, pp. 1-108.

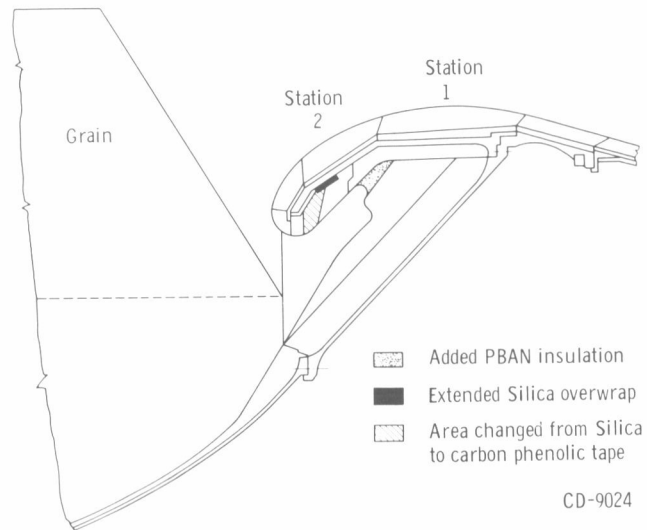


Figure 1. - Modifications to SL-3 nozzle.

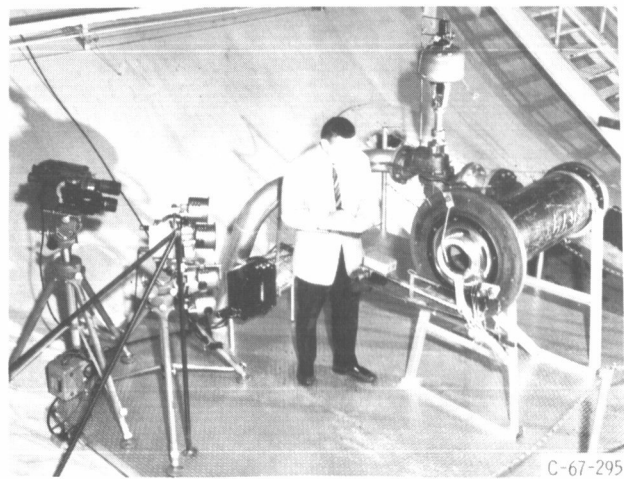
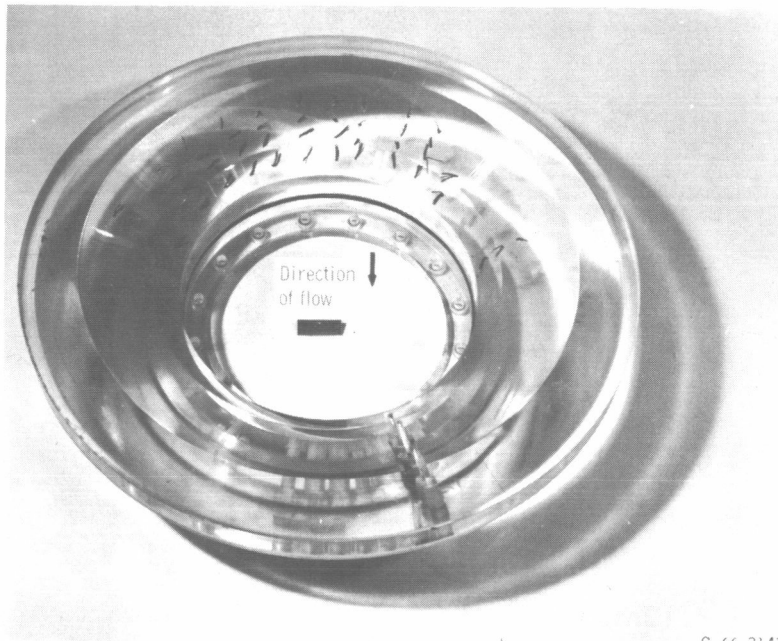
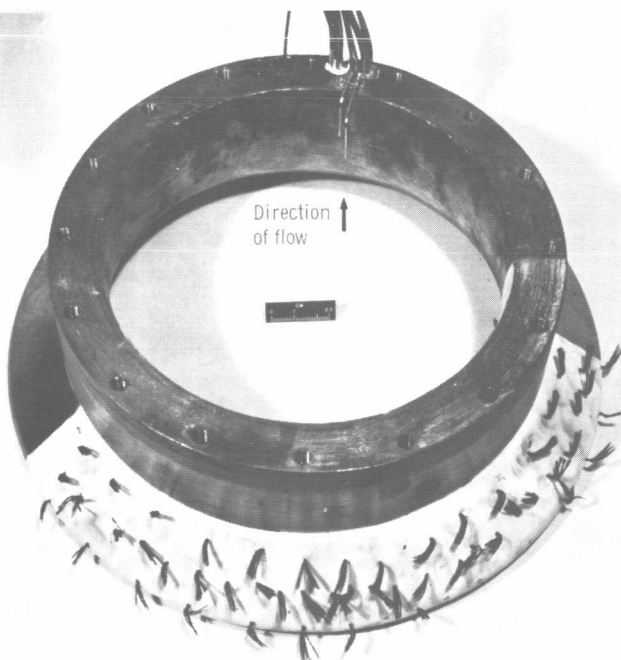


Figure 2. - Model setup in atmospheric test facility.



C-66-3141

Figure 3. - Model transparent aft-end casing.



C-66-3139

Figure 4. - Model nozzle.

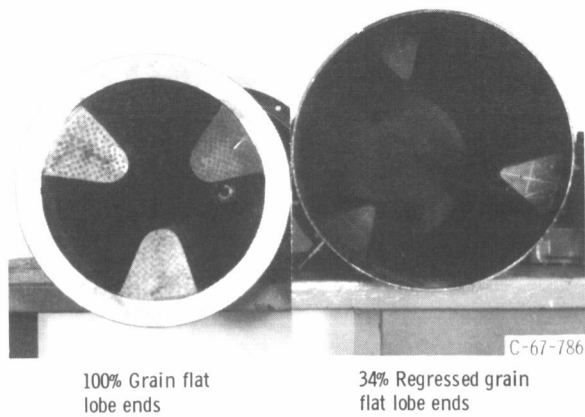


Figure 5. - Simulated propellant grains.

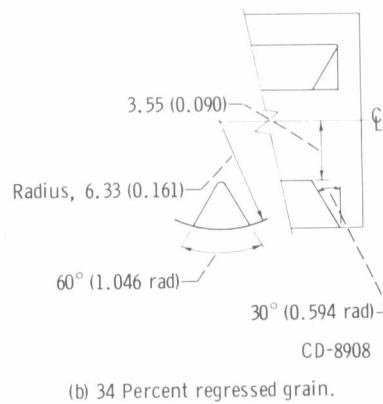
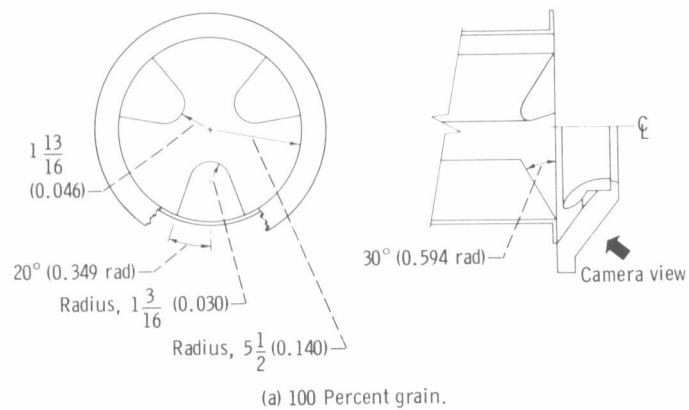
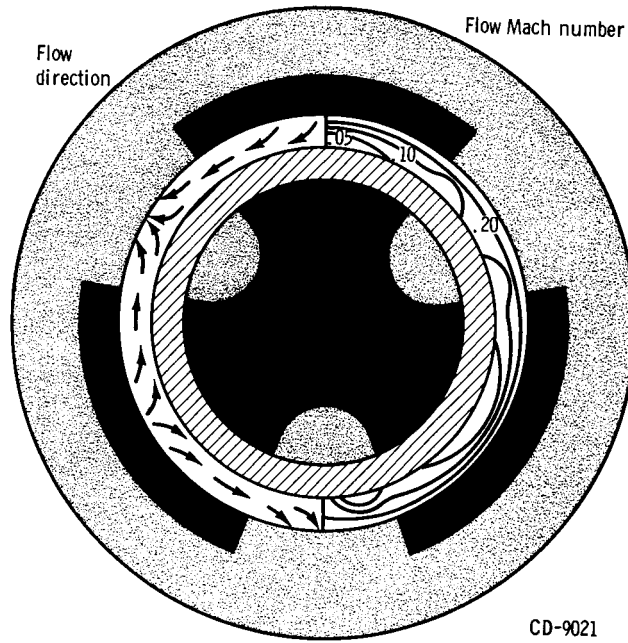
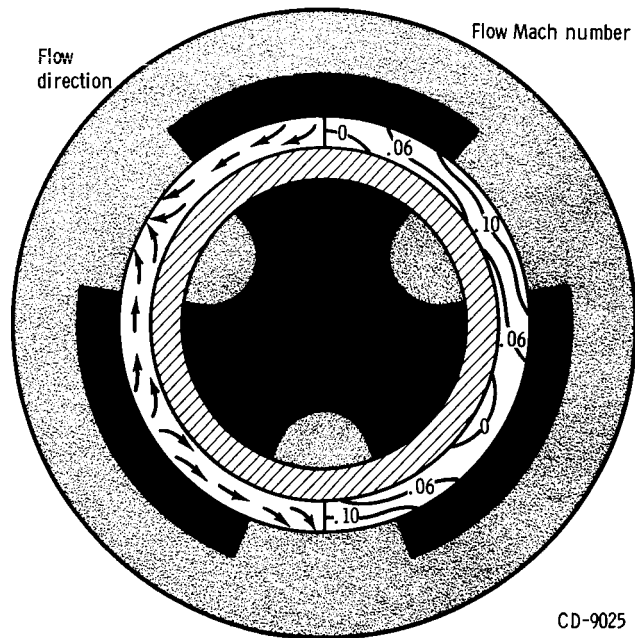


Figure 6. - Geometry of simulated propellant grain configurations. (Linear dimensions in inches (meters).)

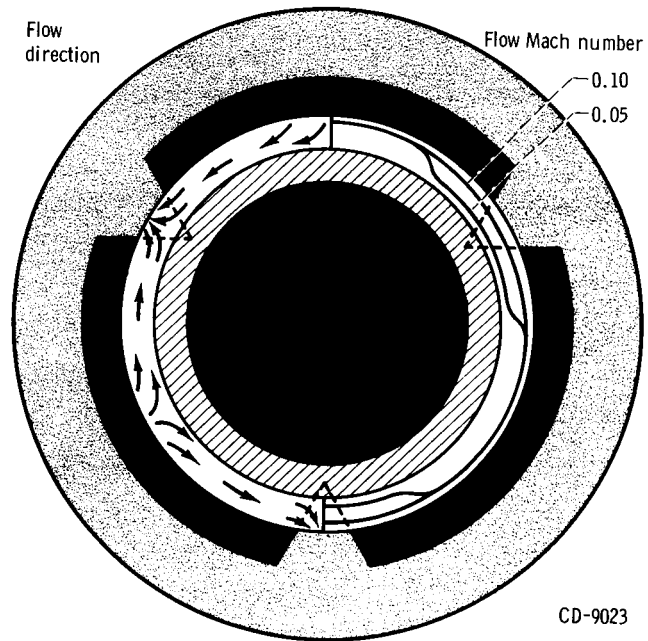


(a) Original nozzle.

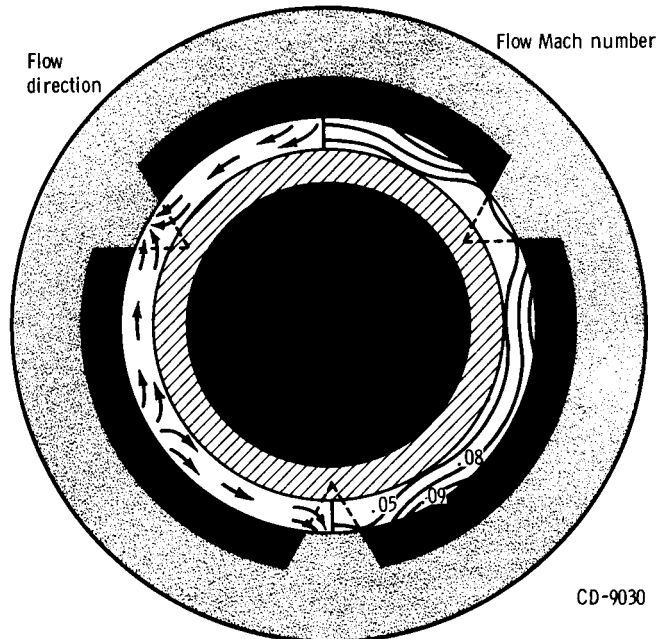


(b) Modified nozzle.

Figure 7. - Annular channel flow characteristics with 100 percent grain.



(a) Original nozzle.



(b) Modified nozzle.

Figure 8. - Annular channel flow characteristics with 34 percent regressed grain.

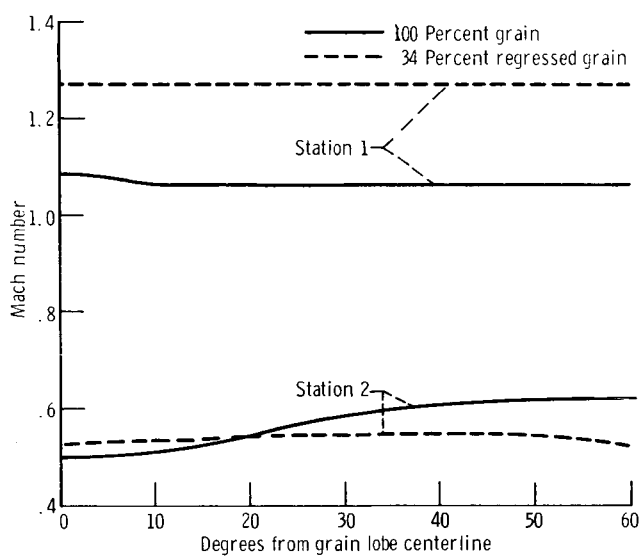


Figure 9. - Circumferential Mach number variation on nozzle surface at two nozzle stations. Station 1 at nozzle throat and station 2 at nozzle area ratio = 1.384.